Pergamon

SCIENCE DIRECT

Bioorganic & Medicinal Chemistry Letters 13 (2003) 3831–3834

BIOORGANIC & MEDICINAL CHEMISTRY LETTERS

# Ganglioside GM1 Mimics: Lipophilic Substituents Improve Affinity for Cholera Toxin

Daniela Arosio, Sergio Baretti, Stefania Cattaldo, Donatella Potenza and Anna Bernardi*

*Dipartimento di Chimica Organica e Industriale, Universita' di Milano, via Venezian 21, 20133 Milan, Italy*

Received 19 May 2003; revised 22 July 2003; accepted 23 July 2003

**Abstract**—Ganglioside GM1 mimics including (*R*)-2-hydroxy-3-cyclohexylpropionic acid or (*R*)-2-hydroxy-3-phenylpropionic acid as replacements for NeuAc are stronger cholera toxin binders than the parent ligand **2**, which includes (*R*)-2-hydroxy-propionic acid.


The use of sugar mimics to antagonize oligosaccharides at the protein receptor level is attracting a great deal of attention as a way to develop drugs with good stability and synthetic availability.[1] Our group has been working in this area using the cholera toxin/ganglioside GM1 (CT/GM1) recognition pair as a model system.[2] In this context, we have described the rational design and the synthesis of the pseudo-oligosaccharide **1**[3,4] (Chart 1), which was found to be as active as the GM1 oligosaccharide (o-GM1, Chart 1) in binding to CT.[3] More recently, we have reported three second-generation mimics[5] obtained by replacing the sialic acid (NeuAc) moiety of **1** with simple α-hydroxyacids, such as (*R*)- and (*S*)-lactic acid and glycolic acid. The most active compound of this series ($K_d = 190$ μM) was **2**, which includes the (*R*)-lactic acid [(*R*)-2-hydroxy propionic acid] side chain (Chart 1).[5,6] NMR data and computer modeling of the second generation ligands have suggested that they are rather flexible in the hydroxyacid region.[7] A similar analysis carried out on their complexes has shown that the protein selects for binding the side-chain conformation which reproduces the orientation of the NeuAc carboxy group in GM1.[7,8] The higher affinity of **2** relative to the other ligands of the series appears to result from van der Waals interactions established between its side-chain methyl group and the toxin cleft. This information suggests that the affinity of the pseudo-GM1 binders may be improved by adding appropriate hydrophobic fragments to the framework of the (*R*)-lactic acid GM1-mimic **2**.

Here, we report that indeed the pseudo-GM1 ligands **3** and **4**, which include a cyclohexyl group and a phenyl group, respectively, do display stronger affinity for CT than **2**. Remarkably, the (*R*)-2-hydroxy-3-phenyl propionic acid derivative **4** with a 10-μM dissociation constant is just one order of magnitude less potent than the natural ligand o-GM1[9] against the cholera toxin.

The two new ligands were synthesized by minor modifications of the established sequence,[5] as reported in Scheme 1. Starting from the enantiomerically pure diol **5**[4,10] the monoethers **8** and **9** were synthesized by $Bu_2SnO$-mediated regioselective alkylation[11] using the triflates **6** and **7**,[6] respectively. TfOH promoted glycosylation of the axial hydroxy group with the Galβ1-3GalNAc donor **10**[4] gave the protected pseudo-trisaccharides **11** and **12**. Standard removal of the protecting groups yielded **3** and **4**.[12]

The interaction of the ligands with the cholera toxin B5 pentamer (CTB) was studied using the intrinsic fluorescence of the Trp88 residue in the toxin binding site. Ligand binding to CTB is known to induce bathochromic shifts and variations in fluorescence intensity whose extent depends on the structure of the ligand.[9,13,14] The titrations were performed by irradiating the sample at 280 nm, and collecting the data at the maximum of the Trp emission curve, at ca. 350 nm. The normalized changes in the fluorescence emission

*Corresponding author. Tel.: +39-02-5031-4092; fax: +39-02-5031-4072; e-mail: anna.bernardi@unimi.it

0960-894X/$ - see front matter © 2003 Elsevier Ltd. All rights reserved.
doi:10.1016/j.bmcl.2003.07.007

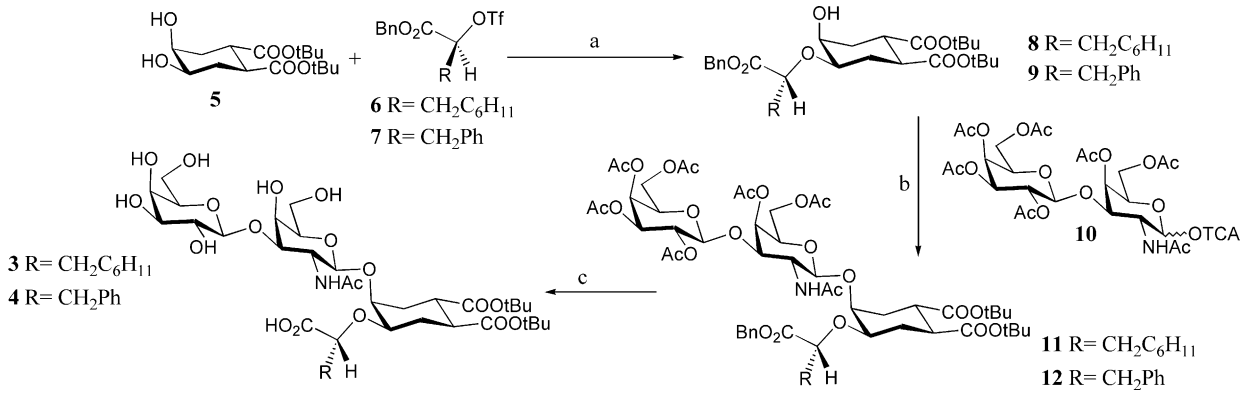


**Scheme 1.** General sequence for the synthesis of **3** and **4**: (a) $Bu_2SnO$, benzene, reflux, then CsF, DME and **6**, or **7** (30% yield); (b) **10** (0.5 equiv) and TfOH (0.05 equiv) in $CH_2Cl_2$, rt to reflux (20%); (c) $H_2$/Pd/C, MeOH (80%); cat MeONa in MeOH (90%).

intensity of CTB upon titration with **2**–**4** are collected in Figure 1. In contrast with GM1 and ps-GM1 **1**, ligands **2**–**4** (Fig. 1) do not display cooperative binding behavior. The dissociation constants determined by non-linear regression analysis are 190 μM for **2**,[5] 45 μM for **3**, and 10 μM for **4**. Thus, it appears that the inclusion of a larger, more lipophilic alkyl group on the hydroxyacid side chain does indeed improve the affinity of the pseudoGM1 binders by up to an order of magnitude. The phenyl group displays a stronger effect than the cyclohexyl group.

In order to rationalize these results, NMR studies on the solution conformation of ligands **3** and **4** were performed by measuring their NOESY and T-ROESY[15] spectra in $D_2O$ solution. The flexibility and orientation of the hydroxyacid chain can be established by examining the NOE interactions for the proton HL, α to the carboxy group, to H-3, H-4 and H-2eq of the cyclohexanediol residue (CHD) (Fig. 2). The results for the (*R*)-2-hydroxy-3-cyclohexylpropionic derivative **3** closely match those already described for the parent compound **2**.[7] Thus, the HL proton shows a set of comparable crosspeaks with CHD-H3 and CHD-H4, and a weaker interaction with CHD-H2eq (Fig. 3). This is consistent with the presence of two orientations of the carboxy group relative to the adjacent diol, which can be idealized as in the Newman projections of Figure 2c and d. One of these, **2d**, which mimics the carboxy group orientation in bound GM1,[8] is presumably the bioactive one.[7]

In contrast, the (*R*)-2-hydroxy-3-phenylpropionic acid derivative **4** appears to be significantly less flexible than **3** and **2** in the side-chain region. In fact, in the ROESY spectrum of **4** only the HL/CHD-H3 and HL/CHD-H2eq crosspeaks are seen, whereas the HL/CHD-H4 crosspeak is not observed (Figs. 2b and 4a). This is consistent with the presence of only one major orienta-

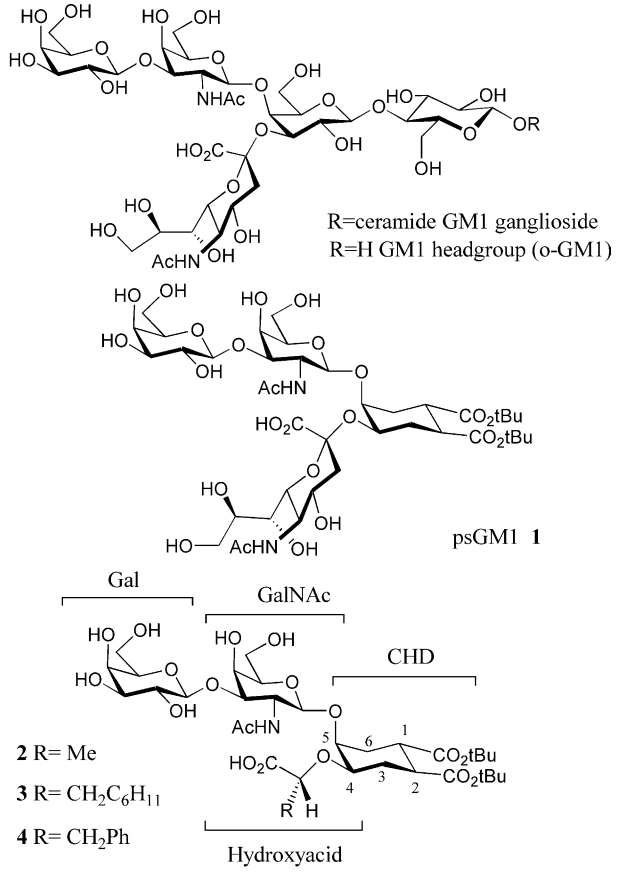


**Chart 1.** Ganglioside GM1 headgroup, the pseudo-GM1 mimic **1**, and the (*R*)-hydroxyacid ligands **2**–**4**.

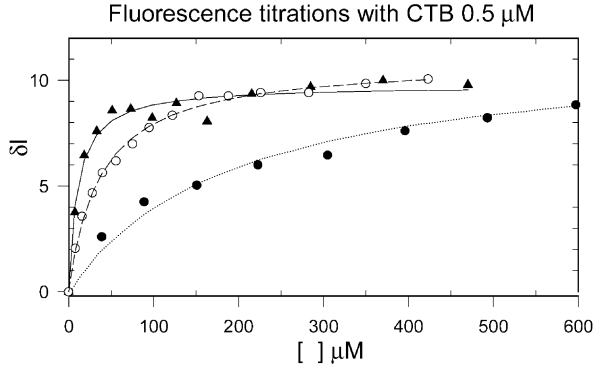


**Figure 1.** Effects of ligand binding on the fluorescence intensity of Trp88 emission in CTB. CTB (0.5 μM) was titrated with micromolar amounts of **2** (black circles, dotted line), **3** (empty circles, dashed line) and **4** (black triangles, solid line). The ligand concentration is plotted against the normalized, absolute value of the relative fluorescence intensity (|δI|) measured at the emission maximum of Trp88.

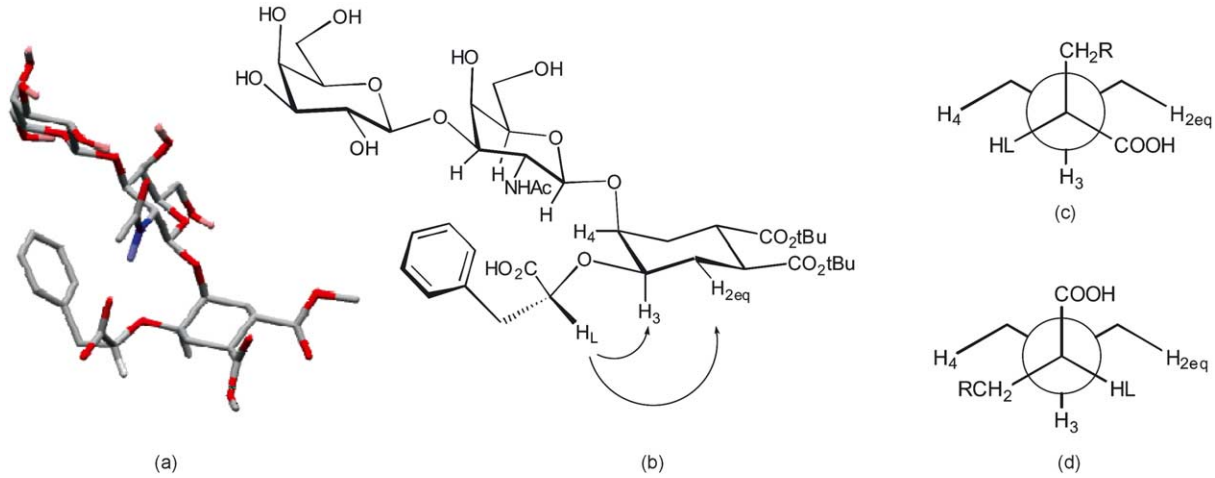


**Figure 2.** Solution solution conformation of the ligands: (a) computer generated 3D structure of **4**; (b) structure of **4**, showing the NOE contacts observed for HL; (c) and (d) Newman projections through the hydroxyacid side chain: both (c) and (d) are populated by **3**, only (d) is populated by **4** (see text).

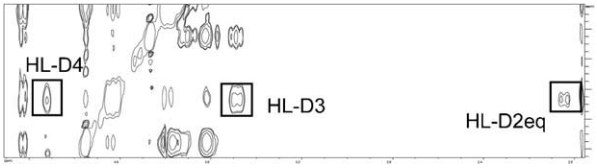


**Figure 3.** T-ROESY spectrum of **3** in $D_2O$ NOEs between the side-chain proton HL and H-4, H-3H-2eq of the ciclohexanediol residue.

tion of the side chain, corresponding to the bioactive idealized Newman projection of Figure 2d. Therefore, contrary to **2** and **3**, ligand **4** appears to be preorganized for toxin binding.

Although more work is required to understand the mode of binding of these ligands, the results reported here suggest that lipophilic groups on the hydroxy acid side chain can contribute to the interaction with CT and that the almost 5-fold increase in affinity of compound **4** over **3** may be interpreted as a result of ligand preorganization. Further analysis of the NMR data suggests that the preorganization of **4** may stem from favorable van der Waals interactions between the phenyl ring and the α-face of the GalNAc residue. A close proximity of these two groups is in fact reported by the strong NOE crosspeaks which are detected between the α-face protons of GalNAc (GN1, GN3 and GN5) and the aromatic side-chain residue (Fig. 4b).[16] Molecular modeling[17] of the free ligand **4** yielded the three-dimensional structure depicted in Figure 2a as the best agreement with the available experimental data. Face-to-face stacking interactions between aminoacid aromatic residues and Gal or GalNAc are frequently observed in experimental sugar–protein complexes.[18] However, to the best of our knowledge, this is the first time that such interaction is observed to occur intramolecularly to stabilize one conformation of a ligand. The results reported here suggest that aromatic/sugar interactions may be used as elements of conformatonal control in the design of glycomimetics.

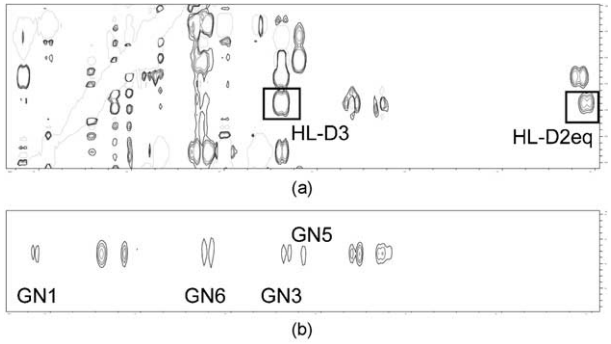


**Figure 4.** T-ROESY spectrum of **4** in $D_2O$: (a) NOE crosspeaks between the side-chain proton HL and the ciclohexanediol residue; (b) crosspeaks observed between the aromatic ring and the GalNAc protons.

Further studies are in progress to determine the mode of binding of **3** and **4** to the cholera toxin.

## Acknowledgements

This work was supported by MIUR and CNR, Istituto di Scienze e Tecnologie Molecolari.

## References and Notes

1. Sears, P.; Wong, C. H. *Angew. Chem.* **1999**, *111*, 2446 Sears, P.; Wong, C. H. *Angew. Chem. Int. Ed.* **1999**, *38*, 2300, and references therein.
2. For a review, see: Bernardi, A.; Arosio, D.; Sonnino, S. *Neurochem. Res.* **2002**, *27*, 539.
3. Bernardi, A.; Checchia, A.; Brocca, P.; Sonnino, S.; Zuccotto, F. *J. Am. Chem. Soc.* **1999**, *121*, 2032.
4. Bernardi, A.; Boschin, G.; Checchia, A.; Lattanzio, M.; Manzoni, L.; Potenza, D.; Scolastico, C. *Eur. J. Org. Chem.* **1999**, *6*, 1311.
5. Bernardi, A.; Carrettoni, L.; Grosso Ciponte, A.; Monti, D.; Sonnino, S. *Bioorg. Med. Chem. Lett.* **2000**, *10*, 2197.
6. For a previous report on the use of hydroxyacids to mimic sialic acid in the context of sialyl-LewisX, see: Kolb, H. C.;

Ernst, B. *Chem. Eur. J.* **1997**, *3*, 1571 In this case, a (*S*)-hydroxyacid was found to be the best replacement for NeuAc.
7. Bernardi, A.; Potenza, D.; Capelli, A. M.; Garcìa-Herrero, A.; Cañada, F. J.; Jiménez-Barbero, J. *Chem. Eur. J.* **2002**, *8*, 4597.
8. Merritt, E. A.; Sarfaty, S.; Jobling, M. G.; Chang, T.; Holmes, R. K.; Hirst, T. R.; Hol, W. G. *J. Protein Sci.* **1997**, *6*, 1516.
9. Schön, A.; Freire, E. *Biochem.* **1989**, *28*, 5019.
10. Bernardi, A.; Arosio, D.; Manzoni, L.; Micheli, F.; Pasquarello, A.; Seneci, P. *J. Org. Chem.* **2001**, *66*, 6209.
11. David, S.; Hanessian, S. *Tetrahedron* **1985**, *41*, 643.
12. **3:** $^1$H NMR ($D_2O$, 400 MHz): 0.91 (m, 2H, CyH-2); 0.14 (m, 4H, CyH-4); 1.38 (s, 9H, $COO(CH_3)_3$); 1.39 (s, 9H, $COO(CH_3)_3$); 1.52–1.69 (m, 9H, CHDH-5ax, CyH-5, $CyCH_2$, CHDH-2ax); 1.93 (s, 3H, $NHCOCH_3$); 2.04 (m, 1H, CHDH-2eq) 2.17 (m, 1H, CHDH-5eq, $J_{5eq-5ax} = 10$ Hz, $J_{5eq-6} \cong J_{5eq-4} = 3.8$ Hz); 2.51 (dt, 1H, CHDH-1, $J_{1-6} \cong J_{1-2ax} = 11.5$ Hz, $J_{1-2eq} = 3.7$ Hz); 2.73 (dt, 1H, CHDH-6, $J_{6-1} \cong J_{6-5ax} = 13.1$ Hz, $J_{6-5eq} = 3.8$ Hz); 3.45–3.52 (m, 2H, CHDH-3, GalH-2); 3.56–3.63 (m, 5H, GalH-3, GalH-5, GalNacH-5); 3.68–3.80 (m, 5H, GalH-6, GalH-6′, GalNAcH-6, GalNAcH-6′, GalNacH-3); 3.96 (d, 1H, GalH-4, $J_{G4-G3} = 3.2$ Hz); 4.03 (m, 2H, GalNAcH-2, $CH_L$); 4.14 (d, 1H, GalNAcH-4, $J_{GN_4-GN_3} = 3.1$ Hz); 4.32 (bs, 1H, CHDH-4); 4.43 (d, 1H, GalH-1, $J_{G1-G2} = 7.8$ Hz); 4.97 (d, 1H, GalNAcH-1, $J_{GN_1-GN_2} = 8.5$ Hz). $^{13}$C NMR-HETCOR ($D_2O$, 400 MHz): 22.8; 26.1; 26.2; 27.5; 28.4; 33.0; 33.4; 34.0; 40.4; 40.6; 44.7; 52.1; 61.2; 68.6; 69.2; 71.0; 72.5; 72.6; 72.7; 75.3; 78.4; 79.6; 80.4; 101.4; 105.5.
**4:** $^1$H NMR ($D_2O$, 400 MHz): 1.36 (s, 9H, $COO(CH_3)_3$); 1.38 (s, 9H, $COO(CH_3)_3$); 1.43 (m, 1H, CHDH-5ax); 1.46 (m, 1H, CHDH-2ax); 1.92 (s, 3H, $NHCOCH_3$); 2.04 (m, 1H, CHDH-2eq) 2.09 (m, 1H, CHDH-5eq); 2.43 (dt, 1H, CHDH-1, $J_{1-6} \cong J_{1-2ax} = 12$ Hz, $J_{1-2eq} = 3.6$ Hz); 2.63 (dt, 1H, CHDH-6, $J_{6-1} \cong J_{6-5ax} = 12$ Hz, $J_{6-5eq} = 3.7$ Hz); 2.92 (dd, 1H, $PhCH_2$-a, $J_{gem} = 14$ Hz, $J_{CH_2a\text{-}HL} = 7$ Hz); 3.05 (dd, 1H, $PhCH_2$-b, $J_{gem} = 14$ Hz, $J_{CH_2b\text{-}HL} = 4.5$ Hz); 3.28 (m, 1H, GalNAcH-5); 3.35 (m, 2H, GalNAcH-3, CHDH-3); 3.45 (dd, 1H, GalH-2, $J_{G_2-G_1} = 7.6$ Hz, $J_{G_2-G_3} = 10$ Hz); 3.59 (dd, 1H, GalH-3, $J_{G_3-G_2} = 10$ Hz, $J_{G_3-G_4} = 3$ Hz); 3.65 (m, 5H, GalH-5); 3.68 (m, 1H, GalH-6); 3.7 (m, 2H, GalNacH-6, GalNAcH-6′); 3.72 (m, 1H, GalH-6′); 3.88 (d, 1H, GalH-4, $J_{G_4-G_3} = 3$ Hz); 3.92 (dd, 1H, GalNAcH-2, $J_{GN_2-GN_1} = 8.6$ Hz, $J_{GN_2-GN_3} = 11$ Hz); 4.01 (d, 1H, GalNAcH-4, $J_{GN_4-GN_3} = 3$ Hz); 4.07 (bs, 1H, CHDH-4); 4.17 (dd, 1H, $CH_L$, $J_{HL-CH_2a} = 7.4$ Hz, $J_{HL-CH_2b} = 4.5$ Hz); 4.35 (d, 1H, GalH-1, $J_{G_1-G_2} = 7.6$ Hz); 4.47 (d, 1H, GalNAcH-1, $J_{GN_1-GN_2} = 8.6$ Hz); 7.28–7.35 (m, 5H). $^{13}$C NMR-HETCOR ($D_2O$, 400 MHz): 22.3; 27.2; 28.5; 33.1; 39.1; 40.9; 44.9; 51.8; 61.0; 61.5; 68.5; 69.0; 71.1; 72.8; 73.2; 74.9; 75.3; 78.6; 80.5; 81.2; 101.7; 105.2; 128.8.
13. Mertz, J. A.; McCann, J. A.; Picking, W. D. *Biochem. Biophys. Res. Commun.* **1996**, *226*, 140.
14. The cholera toxin B5 pentamer (SIGMA®) was resuspended to give the desired concentration in 0.1 M TRIS, 0.4 M NaCl, 2 mM $Na_2EDTA$, 6 mM $NaN_3$, pH 7.5. Fluorescence measurements were made at room temperature with a Perkin–Elmer LS-50 spectrofluorometer. The excitation wavelength was 280 nm, and the spectrum was recorded between 300 and 450 nm.
15. Hwang, T. L.; Shaka, A. J. *J. Am. Chem. Soc.* **1992**, *114*, 3157. Hwang, T. L.; Shaka, A. J. *J. Magn. Res. Ser. B* **1993**, *102*, 155.
16. No analogous crosspeaks were detected between the GalNAc α protons and the cyclohexyl ring in **3**.
17. A conformational search was performed using the MC/EM protocol of Macromodel 7.0, the AMBER* force field, and the GB/SA water solvation model, as described in ref 7. The parameters developed by Kolb and Ernst (from ref 6) were used for the hydroxyacid fragment. For a description of Macromodel, see: Mohamadi, F.; Richards, N. G. J.; Guida, W. C.; Liskamp, R.; Lipton, M.; Caufield, C.; Chang, G.; Hendrickson, T.; Still, W. C. *J. Comp. Chem.* **1990**, *11*, 440.
18. (a) Weis, W. I.; Drickamer, K. *Annu. Rev. Biochem.* **1996**, *65*, 441. (b) Elgavish, S.; Shaanan, B. *J. Mol. Biol.* **1998**, *277*, 917. (c) Quiocho, F. A. *Annu. Rev. Biochem.* **1986**, *55*, 287. (d) Vyas, N. K. *Curr. Opin. Struct. Biol.* **1991**, *1*, 732. (e) Quiocho, F. A. *Biochem. Soc. Trans.* **1993**, *21*, 442.